PHILOSOPHICAL TRANSACTIONS OF THE ROYAL SOCIETY A MATHEMATICAL, PHYSICAL & ENGINEERING SCIENCES

Room-temperature molecule-based magnets

Michel Verdaguer, , , , and

Phil. Trans. R. Soc. Lond. A 1999 **357**, 2959-2976
doi: 10.1098/rsta.1999.0476

THE ROYAL SOCIETY

Room-temperature molecule-based magnets

By Michel Verdaguer, A. Bleuzen, C. Train, R. Garde, F. Fabrizi de Biani and C. Desplanches

Laboratoire de Chimie Inorganique et Matériaux Moléculaires, Unité Associée au CNRS 7071, Case 42, Université Pierre et Marie Curie, 75252 Paris Cedex 05, France

Room-temperature magnets belonging to the Prussian blue family were obtained recently through mild chemistry methods, i.e. molecular solution chemistry at room temperature and pressure. The paper describes the rational way followed to reach this goal and the prospects opened. First, the structure of Prussian blues and how it allows variation of the electronic structure and exchange interaction through the cyanide bridge is recalled. Then it is shown how the systematic use of orbital models and simple semiempirical calculations, combined with the Néel molecular field approach, helps in increasing the Curie temperature up to room temperature in vanadium–chromium derivatives. Some methods are then proposed to improve the magnetic properties and some examples of applications in demonstrators, devices, photomagnetism, etc, are given. Finally, we mention some exciting challenges in molecular magnetism, including the preparation of single molecule magnets at room temperature.

Keywords: Prussian blue analogues; molecule-based magnets; hexacyanometallates; vanadium–chromium system; thin layers; devices

1. Introduction

Ten years ago, writing a paper with such a title would have been impossible: no room-temperature molecule-based magnet was available on the molecular market. Many efforts in this direction had been made with some remarkable achievements, both theoretical and experimental, which have been reported in conference proceedings (see Güdel 1985; Miller *et al*. 1989; Gatteschi *et al*. 1991), but it was necessary to wait until 1991 to read the first report, by Miller and coworkers (see Manriquez *et al*. 1991), of a room-temperature molecule-based magnet. Since then, a rapid development of the field has taken place, thanks to the endeavours of inorganic chemists engaged in molecular magnetism and particularly in the synthesis of systems with a tunable three-dimensional magnetic ordering temperature T_C. This allows the presentation of some examples and prospects.

One of the driving forces of such fundamental research is the need for high-density storage materials: the molecular level is indeed the ultimate step for storage capacity. Moreover, the accessibility of polyfunctional materials may answer some unsolved technological problems. Truly, in the field of materials, molecular chemistry is expected to present several drawbacks: the solids are diluted, their mechanical properties are often weak and their thermal stability is low. However, this is compensated by many other advantages: solubility in various solvents and the ability to

crystallize beautiful complex structures; the uniform character of the structures and properties of the molecules; the frequent biocompatibility; the low density; the optical properties (transparency, etc.); and the ability to present cofunctions (magnetism and optics, conductivity and magnetism, etc.). Some of the reasons that convinced chemists of the possibility of working in this direction are also related to the feasibility of working in 'mild chemistry' conditions; that is, to easily realize experiments in solution at room temperature and pressure.

A strong theoretical corpus relies on the ligand field theory and on the mechanisms of the interactions between neighbouring unpaired electrons in a molecule or in a solid. The existence of various correlations between structures and properties facilitates the prevision of the physical properties and of the related structures and is another strong argument to attract scientists to this field. It is therefore not surprising to encounter an active community trying different steps to cover the domain from the isolated complex to the three-dimensional ordered magnet.

In the present paper we describe our approach to room-temperature magnets using old-fashioned Prussian blue analogues, but looking at them with new eyes. The nature of the exchange interaction in these materials is discussed to explain the strategy developed to obtain room-temperature magnets. The experimental endeavours to improve the properties of room-temperature magnets are then presented. The use of these compounds in devices, their synthesis as thin films and, finally, a prospective concerning single-molecule magnets concludes the paper.

2. How to get room-temperature magnets?

Everyday life is full of examples of useful room-temperature metallic or oxide magnets. Our purpose is not to reproduce or to expand such results by high-temperature preparations of metals, alloys or oxides. Our challenge is to start from molecules, existing as such in solution, suitably designed to build a magnetic solid where intermolecular interactions are strong enough in the three directions of space for the magnetic ordering to survive at room temperature.

Three situations may arise in a molecule-based solid:

(A) the molecules are neutral, independent, with weak van der Waals interactions between them—the solid is truly molecular, the cooperativity is weak;

(B) the molecules are charged and well insulated from each other by counterions—the solid is made of molecular ions, the cooperativity is weak;

(C) the molecules have strong interactions between each other (bonding and exchange)—the cooperativity is strong.

Figure 1 shows the Lewis acid–base interaction between two molecules in case (C). An important feature is that most frequently the unpaired 'magnetic' electrons are non-bonding or antibonding electrons.

In this way it is possible, on the one hand, to design the molecular precursor by choosing the metallic ions (electronic structure, charge, spin), the nature of the ligands (charge, bonding, spin), the nature of the metal–ligand interaction and therefore the ligand field. This flexibility is the one of molecular chemistry. On the other hand, it is possible to combine the molecular precursors with different assembling units:

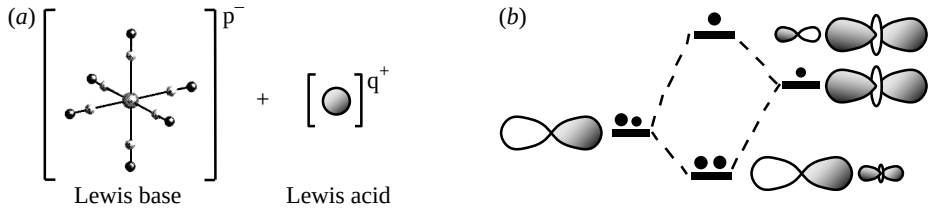

Figure 1. Schematic representation of Lewis acid–base interactions using hexacyanometallate and paramagnetic cations: (*a*) structural model; (*b*) orbital interaction.

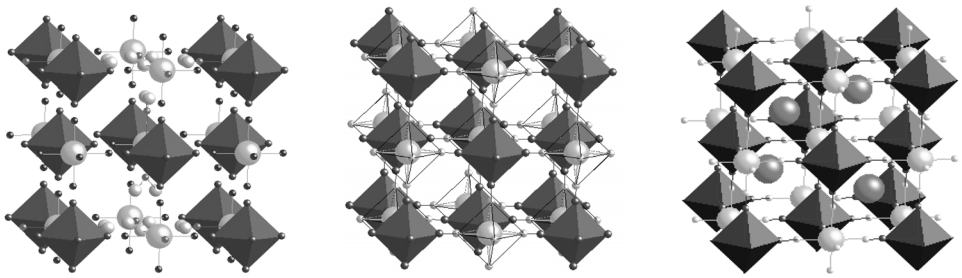

Figure 2. Typical structures of cubic Prussian blue analogues: (*a*) $M_3'^{II}[M^{III}(CN)_6]_2$, nH_2O, $M_3'M_2$; (*b*) $M'^{III}[M^{III}(CN)_6]$, $M_1'M_1$; (*c*) $CsM'^{II}[M^{III}(CN)_6]$, $Cs_1M_1'M_1$.

the resulting periodical crystal structure allows the chemist to play with the vacancies and the doping. This flexibility is the one of solid-state chemistry. We chose the polycyanometallates $[M(CN)_n]^{p-}$ as the molecular precursors ten years ago since we found several of their properties promising. Indeed, they have a large structural flexibility, from one to eight coordination positions, and they have a wide coordination chemistry, being good Lewis bases. They are soluble in water, generally very stable and, some of them, especially with d^3 and d^6 ions, are quite inert; all these conditions are required to avoid secondary reactions of the cyanide ligand. The cyanide ligand is amphiphilic and allows the binding of different metallic ions on the two sites. Polycyanometallates allow the preparation of three-dimensional networks through the easy precipitation of neutral solids from solution. The overall symmetry of the bimetallic systems obtained from polycyanometallates is easy to control: the very symmetric isotropic cubic Prussian blues derived from the octahedral $[M(CN)_6]^{p-}$ analogues are well known (see Ludi & Güdel 1973); nevertheless, anisotropic and lower symmetry precursors like $[M(CN)_7]^{p-}$ or $[M(CN)_8]^{p-}$ lead to more intricate three-dimensional structures (see Larionova *et al*. 1998).

Our first attempts focused mainly on *hexacyanometallates* since the octahedral $[M(CN)_6]^{p-}$ precursors allow one to develop interactions with six neighbours in the three directions of space. They give rise to highly symmetrical systems, allowing the nature of the interactions in the linear arrangement M—CN—M′ to be understood. They span a large range of M/M′ stoichiometries, thanks to the choice of the charges on M and M′, and this is further increased by the possible insertion of monovalent cations in the tetrahedral sites of the structure (figure 2).

The T_C of the Prussian blue $Fe_4^{III}[Fe^{II}(CN)_6]_3 \cdot 14H_2O$ was measured as $T_C = 5.6$ K (see Ito *et al*. 1968). Replacing Fe^{III} and Fe^{II} by other transition metal ions,

in a systematic study of three-dimensional cyanides, Babel, at Marburg university, demonstrated that an ordering temperature above liquid nitrogen could be reached: the highest T_C was obtained with the ferrimagnet $CsMn^{II}[Cr^{III}(CN)_6]$, $T_C = 90$ K (see Babel 1986). One of the key points in Babel's study is the use of two neighbouring paramagnetic ions M and M′ in the lattice, otherwise a paramagnetic system is obtained.

A short-range ferromagnetic coupling leads to a total spin ground state which is the sum of the spins: $S_T = S_A + S_B$; a short-range ferromagnetic coupling leads to a total spin ground state which is the difference of the spins: $S_T = |S_A - S_B|$. The key point is that antiferromagnetism between two neighbours bearing different spins leads to a magnetic ground spin state, known as ferrimagnetism after Néel (see Néel 1948). The ground-state spin value is less than when the coupling is ferromagnetic, but it is amazing to observe that orbital overlap can transform a phenomenon (antiferromagnetism) into the opposite phenomenon (magnetism) in a dialectic process.

To demonstrate the feasibility of the molecular approach to high-T_C systems, we used two theoretical tools: (*a*) the molecular field, proposed by Néel in three-dimensional systems and well known among physicists and solid-state chemists (see Néel 1948; Herpin 1968; Goodenough 1963); and (*b*) the orbital model of exchange interaction designed by Kahn for molecular chemistry (see Girerd *et al.* 1981; Kahn 1993).

In Néel (1948) an expression is given of the susceptibility of an AB ferrimagnet near the ordering temperature from which we can deduce

$$kT_C = \frac{Z|J|}{N_A g^2 \beta^2} \sqrt{C_A C_B}, \tag{2.1}$$

where Z is the number of magnetic neighbours, $|J|$ is the absolute value of the exchange interaction, C_A and C_B are the Curie constants of A and B, N_A is the Avogadro constant, g is a mean g Landé factor and β is the Bohr magneton. Everything being equal, to increase T_C, it is therefore necessary to enhance Z, $|J|$ and the Curie constants C_A and C_B ($C_i = S_i(S_i + 1)$, if S_i is the spin of site i).

Z is controlled by the stoichiometry; with hexacyanometallates its maximum is 6 when the ratio M′/M is 1; its average becomes 4 when $M'/M_{2/3}$. More generally, for M'/M_z, $Z = 6z$ and one easily finds that $T_C(M'/M_z) = zT_C(M'/|MM)$.

To foresee the $|J|$ value, Hoffmann's orthogonalized magnetic orbitals model (see Hay *et al.* 1975) or Kahn's magnetic orbitals model can be used. Both models predict that orthogonal orbitals give rise to ferromagnetism and that orbital overlap gives rise to antiferromagnetism. Due to its better versatility with asymmetric systems we prefer to use Kahn's model. The following expression summarizes the model in the case of two electrons on two sites, described by two identical orbitals: the singlet–triplet energy gap, equal to J ($J = E_S - E_T$), is given by

$$J = 2k + 4\beta S. \tag{2.2}$$

Here k is the bielectronic exchange integral (positive) between the two non-orthogonalized magnetic orbitals a and b, β is the monoelectronic resonance integral (negative) and S is the monoelectronic overlap integral (positive) between a and b. The positive term represents the ferromagnetic contribution J_F, favouring parallel alignment of the spins, while the negative term is the antiferromagnetic contribution J_{AF}, favouring antiparallel alignment of the spins. When the two a and b orbitals are different, in

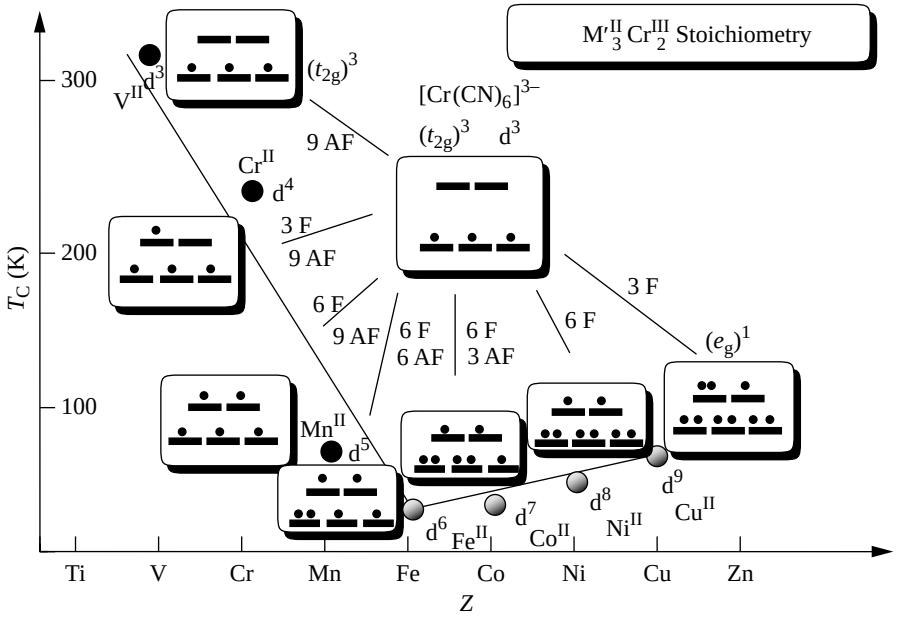

Figure 3. Exchange pathways in a binuclear [Cr^{III}—CN—M′^{II}] linear unit when M′^{II} is a divalent ion of the first period of the transition metals and $T_C = f(Z_{M'})$ in related M′$_3^{II}$Cr$_2^{III}$ systems.

the absence of a rigorous analytical treatment, the semiempirical relation proposed by Kahn can be used (see Kahn 1993):

$$J = 2k + 2S(\Delta^2 - \delta^2)^{1/2}, \tag{2.3}$$

where δ is the initial energy gap between the magnetic orbitals and Δ is the energy gap between the molecular orbitals derived from them.

When several electrons are present on each centre, n_A on one side, n_B on the other, J can be described by the sum of the different 'orbital pathways', $J_{\mu\nu}$, weighted by the number of electrons (see Kahn 1993):

$$J = (\Sigma_{\mu\nu} J_{\mu\nu})/n_A n_B. \tag{2.4}$$

The kind and the number of orbital interactions between the magnetic orbitals of M (t_{2g} local symmetry) and M′ (t_{2g} and e_g local symmetries) in the linear arrangement M—C≡N—M′ are described in figure 3, where M is Cr^{III} and $(t_{2g})^3$ and M′ are the divalent cations of the first period of transition metal ions.

It is clear from this simple scheme that ferromagnetic interactions can be expected with M′ = Cu^{II} and Ni^{II}, weak interactions with Co^{II} and Fe^{II} and stronger and stronger antiferromagnetic interactions from Mn^{II} to V^{II}. The experimental results in the M′$_3^{II}$Cr$_2^{III}$ stoichiometry series confirm the predictions of the model: the Cu^{II} and Ni^{II} derivatives are indeed ferromagnetic (see Gadet *et al.* 1992); the Co^{II} and Fe^{II} derivatives display the lowest T_C. The Mn^{II} analogue is ferrimagnetic (see Babel 1986), a Siberian ambient temperature is reached with Cr^{II} (see Mallah *et al.* 1993) and the first magnetic Prussian blue above European room temperature is obtained with V^{II}, $T_C = 315$ K or 42 °C, ferrimagnetic (see Ferlay *et al.* 1995). A very important point is the magnitude of the ferromagnetic contributions: all the Cr^{III}(CN)$_6$

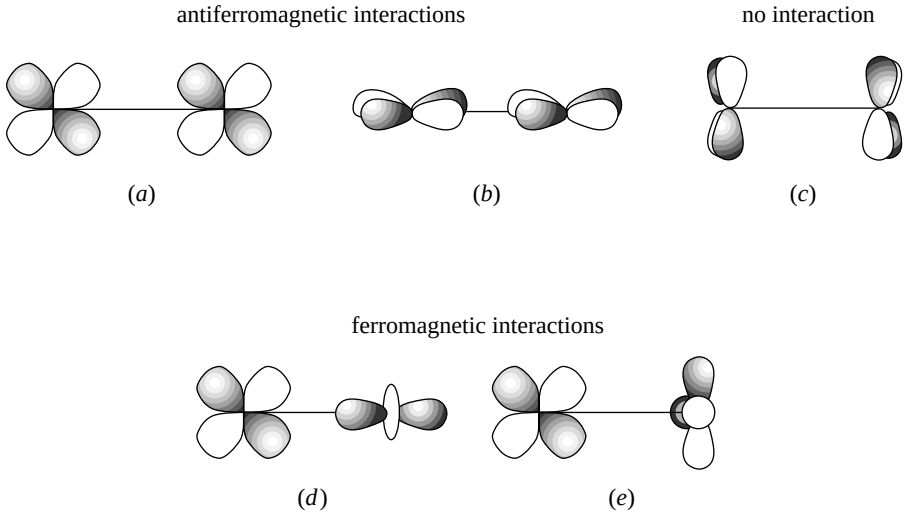

Figure 4. Orbital interactions in a binuclear unit $[(CN)_5M'^{II}(\mu\text{-}NC)M^{III}(CN)_5]^{6-}$.

derivatives with M′ going from Fe^{II} to Ni^{II} are ferromagnetic. When the ferromagnetic contributions are progressively suppressed from Mn^{II} to V^{II}, large antiferromagnetic J values and high T_C are obtained.

The validity of the above simple orbital approach can be confirmed by semiempirical extended Hückel calculations (see Landrum 1992) on a series of heterobinuclear complexes with formula $[(CN)_5M'^{II}(\mu\text{-}NC)M^{III}(CN)_5]^{6-}$ and new insights on the systems are obtained.

Interactions were computed in the binuclear unit $[(CN)_5M^{II}(\mu\text{-}NC)M'^{III}(CN)_5]^{6-}$, where M^{II} = Ti, V, Cr, Mn, Fe, Co and M^{III} = Ti, V, Cr, Mn, Fe, so that there was always at least one antiferromagnetic pathway between M′ and M. We therefore chose M ions possessing no more than five electrons, which occupy the t_{2g} orbitals, and M′ ions possessing no more than seven electrons, so that in a high spin state they also have t_{2g} orbitals that are at least partly filled. Bond distances were kept fixed (M—C = 2.07 Å, C—N = 1.13 Å, M′—N = 2.10 Å) for all the combinations to monitor separately the influence of the electronic configuration.

As shown in figure 4, in the binuclear systems two couples (a and b) of the six t_{2g} orbitals strongly interact, the strength of the coupling being the same. In a three-dimensional network the missing interaction becomes possible (c), as strong as the other ones, so that it can be summed with the others. Due to the symmetry of the system it is sufficient to analyse the interaction for a single couple and to sum up on all the combinations present in a three-dimensional network. Two of the possible interactions between t_{2g} and e_g orbitals (d and e) are also shown in figure 4.

For each pair of metals the value of Δ and δ have been calculated (see equation (2.3)). Some features may be revealed by decomposing the antiferromagnetic term as $(\Delta^2 - \delta^2) = (\Delta - \delta)(\Delta + \delta)$. Two effects contribute to the tendency of the electrons to pair: (i) a strong interaction between the magnetic orbitals is represented by the term $(\Delta - \delta)$; and (ii) a possible charge transfer between the two magnetic orbitals, represented by the term $(\Delta + \delta)$. The dependence of Δ on δ is non-trivial. Δ contains δ itself, but it is enhanced when δ is small, since the orbitals better fit in

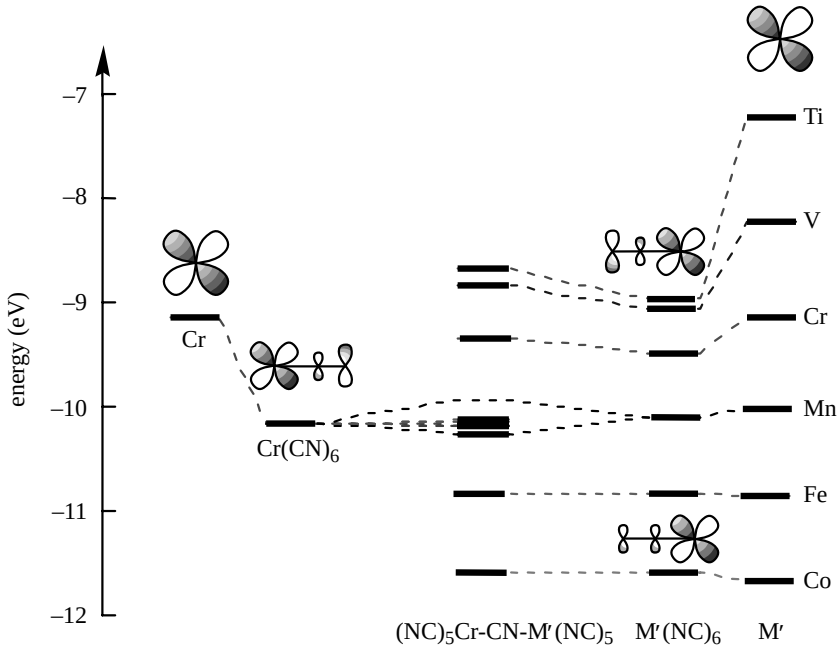

Figure 5. Composition of the magnetic orbitals and variation of π and π^* interactions when M′ is varied.

energy. Therefore, to have a strong antiferromagnetic interaction it is necessary to have the best combination between these two terms, which have opposite constraints: $(\Delta - \delta)$ is higher when δ is smaller, while $(\Delta + \delta)$ is higher when δ is higher. In cases when the interelectronic repulsion on one centre is strong (localized electrons), charge transfer is unlikely and the $(\Delta - \delta)$ becomes the leading term.

Figure 5 shows the interaction between the magnetic orbitals of the $Cr(CN)_6$ and $M'(NC)_6$ moieties. In both halves the t_{2g} orbitals are more or less involved in a back-donation interaction with the empty CN π^* orbitals and in a repulsion interaction with the full CN π orbitals. This double interaction severely affects the energy of the magnetic orbitals, which depends on the diffuseness of the d orbitals of the metallic ions (lower values of the ζ Slater coefficient in our calculation) and on the relative position of the d orbitals with respect to the energy of the π and π^* CN orbitals. For example, in the case presented in figure 5, all the M′ sites from Ti to Cr are mainly involved in a π^* back-donation interaction, while for M′ going from Mn to Co the π repulsion interaction almost compensates the first interaction. Two important consequences follow: (i) it is not obvious which magnetic orbitals will have the best fit in energy; and (ii) the composition of the magnetic orbitals is affected as shown in figure 5, as well as the overlap between them. The stronger interaction generally involves moieties possessing different metals and corresponds to cases where Δ and δ possess their *lower* values.

The corresponding $(\Delta^2 - \delta^2)$ values are shown in figure 6. The higher $(\Delta^2 - \delta^2)$ values are reached for the $[(CN)_5Ti^{II}(\mu\text{-}NC)M^{III}(CN)_5]^{6-}$ binuclear units and, among them, the highest is found for the $[Ti^{II}Fe^{III}]$ pair. Such a result appears counter-intuitive at first sight. It is understood by noting that the better combination for

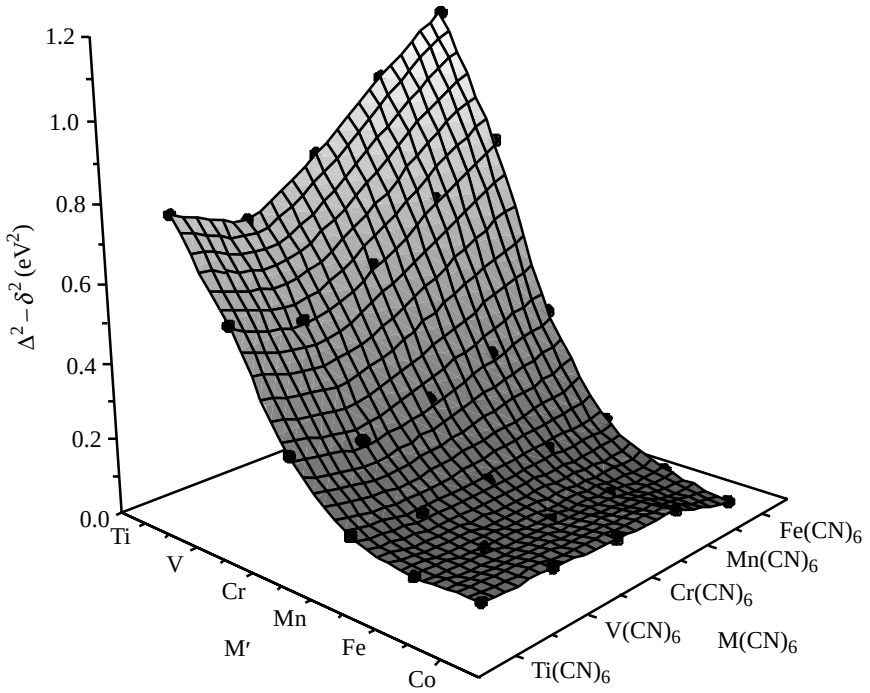

Figure 6. Values of $\Delta^2 - \delta^2$ for the different couples of $[M(CN)_6]$ and M′.

$(\Delta + \delta)$ and $(\Delta - \delta)$ is obtained due to both the high values of Δ and δ and to the diffuseness of the d orbital of Ti, which allows an efficient overlap between the magnetic orbitals (high $\Delta - \delta$). The calculated surface also suggests that the compounds containing an M cation chosen in the first members of the series should always possess the stronger antiferromagnetic interaction, whatever the M′ metal ion chosen.

As foreseen from the Néel expression, the strength of J_{AF} is not the only parameter to determine the T_C value since the number of possible interactions and the spin of both sites affect the critical temperature. Indeed, the product $Z|J|\sqrt{C_{M'}C_M}$ is much more reliable in predicting T_C for the different combinations of M and M′ ions. If we consider $z = 1$ $(Z = 6)$ we obtain, from equation (2.5),

$$T_C \propto \frac{|J|}{N_A g^2 \beta^2}\sqrt{C_M C_{M'}} \propto \frac{N(\Delta^2 - \delta^2)}{n_M n_{M'}}\sqrt{C_{M'}C_M}. \tag{2.5}$$

All the symbols maintain their usual meaning and N is the number of interactions. Since $C_i \propto n_i(n_i + 2)$, we multiplied the data plotted in figure 6 by the factor

$$N\sqrt{\frac{(n_M + 2)(n_{M'} + 2)}{n_M n_{M'}}},$$

so obtaining the surface shown in figure 7.

The result is in good agreement with the experimental values of T_C (see Dunbar *et al.* 1997) and confirms that in these series the best choice is indeed the vanadium–chromium pair.

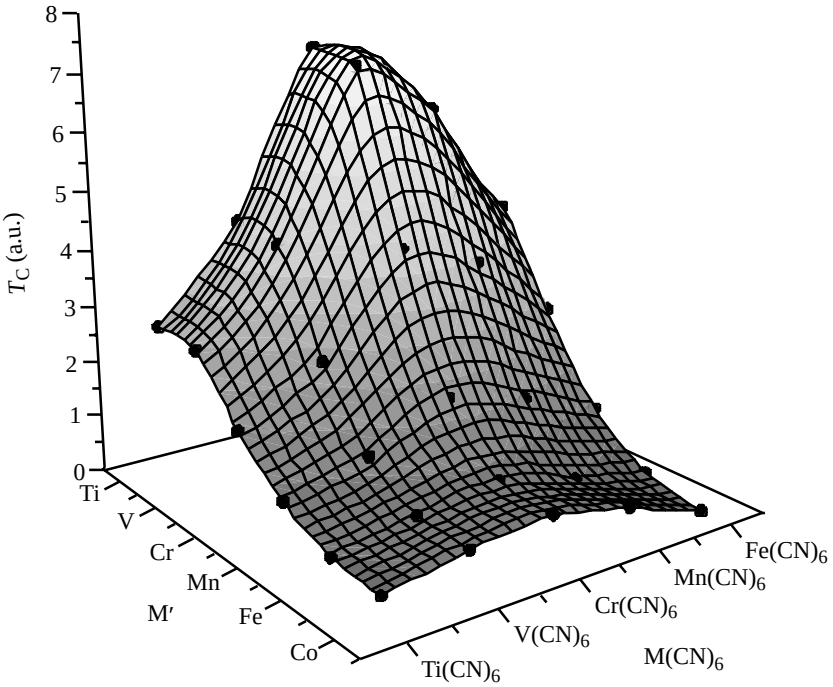

Figure 7. Computed values of T_C (in arbitrary units) when varying M and M′.

The ferromagnetic contributions cannot be explicitly calculated, being bielectronic in origin. Nevertheless, some hints can be attained even from these simple calculations. The exchange integral k_{ab} between two magnetic orbitals $|a\rangle$ and $|b\rangle$ is directly proportional to the squared overlap density $\rho_{ab} = |a\rangle|b\rangle$ (see Charlot & Kahn 1980). This contribution to the exchange interaction is always present and it becomes the only contribution when the overlap S_{ab} is zero, i.e. for the t_{2g}–e_g interactions. For example, in a binuclear complex $[(CN)_5Ni^{II}(\mu\text{-}NC)Cr^{III}(CN)_5]^{6-}$, the $\rho_{t_{2g}-e_g}$ overlap density can be computed and illustrated by the projection on the xz-plane of the product $|(Cr)t_{2g}\text{–}xz\rangle|(Ni)e_g\text{–}z^2\rangle$ of the orbitals of the fragments $Ni^{II}(NC)_6$ and $Cr^{III}(CN)_6$. The orbital composition is given by the extended Hückel output. Figure 8 shows the overlap density between the t_{2g}–xz magnetic orbital centred on chromium and the e_g–z^2 magnetic orbital centred on the nickel and the presence of high overlap density zones. The peak value of ρ is found in the surrounding of the nitrogen atom of the cyanide, which is a peculiar feature of the electronic structure of the cyanide bridge giving rise to strong ferromagnetic interactions, strong positive J values and high T_C.

To close this section we focus on the vanadium–chromium (VCr) system and study the role of the number of interactions when varying the stoichiometry. All the experimentalists working on this system are faced with the problem of the oxidation of vanadium (II) during the reaction. In some cases, a mixed-valence V^{II}–V^{III} system arises; in some other cases vanadyle $V^{IV}O$ is present. The general formula of a V^{II}–V^{III}/Cr^{III} system is written as $(C_yV^{II}_{\alpha}V^{III}_{1-\alpha}[Cr^{III}(CN)_6]_z \cdot nH_2O)$. ($C^I_y$ is a simplified formulation and covers more complex situations corresponding to different cationic or anionic species in the lattice to insure electroneutrality). To arrive at a simpler

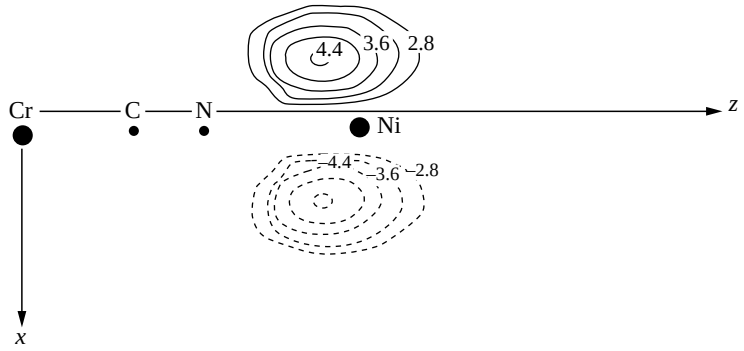

Figure 8. Projection on the xz-plane of the overlap density ρ between the t_{2g}–xz-type magnetic orbital centred on chromium and the e_g–z_2-type magnetic orbital centred on nickel.

representation of the phenomenon, we consider as a first step that the J value of the V^{II}–Cr^{III} pair is the same as the J value of the V^{III}–Cr^{III} pair (see Ferlay *et al.* 1999). In these conditions T_C follows equation (2.6) and depends in a straightforward manner upon the fraction of vanadium (II), α and upon the stoichiometry z:

$$T_C \propto z\sqrt{z}|J|\sqrt{C_{Cr^{III}}}\sqrt{C_V} \propto z\sqrt{z}\sqrt{C_{Cr^{III}}}\sqrt{[\tfrac{7}{4}\alpha - 2]}. \tag{2.6}$$

The surface giving $T_C = f(z, \alpha)$ is shown in figure 9 and demonstrates that the highest T_C is expected for $z = 1$ and $\alpha = 1$, i.e. for the compound $C^{I}V^{II}[Cr^{III}(CN)_6]$. This is a misleading conclusion of course, since $C^{I}V^{II}[Cr^{III}(CN)_6]$ is definitively an antiferromagnet due to the exact cancellation of the $\frac{3}{2}$ spins of the vanadium (II) and chromium (III). Nevertheless, a compound with a composition close to this one is expected to have a T_C close to the predicted maximum.

The above simple calculations and considerations not only allow one to put our simple qualitative orbital model on a firmer basis but also give new tools to improve the magnetic characteristics (T_C, magnetization at saturation, coercivity, etc.) of room-temperature magnets.

3. Attempts to improve the characteristics of room-temperature Prussian blue magnets

We will still stick to the [VCr] system. The first point to raise is that real chemistry is much more complex than any model: the expected $V^{II}_3[Cr^{III}(CN)_6]_2$ is an amorphous non-stoichiometric compound, a deep-blue mixture of V^{II} and V^{III}, $V^{II}_{\alpha}V^{III}_{(1-\alpha)}[Cr^{III}(CN)_6]_{0.86} \cdot 2.8H_2O$, with $\alpha = 0.42$, and very sensitive to air (see Ferlay *et al.* 1995). The magnetization at saturation is very weak ($0.15\mu_B$) in line with the proposed formulation. The coercive field is one of a very soft magnet (25 Oe at 10 K). To try to improve the properties and to obtain better characterized materials, our group and the groups of Girolami, Hashimoto and Miller undertook new syntheses. Many factors play an important role in the successful synthesis of [VCr] analogues with improved magnetic properties. Among them are the oxidation state of the vanadium ions, the stoichiometry and the structure (presence of counterions, solvent, etc.) and the crystallinity and the size of the particles. Today, a set of non-stoichiometric Prussian blue analogues $C^{I}_{y}V[Cr^{III}(CN)_6]_z \cdot nH_2O$ is available with

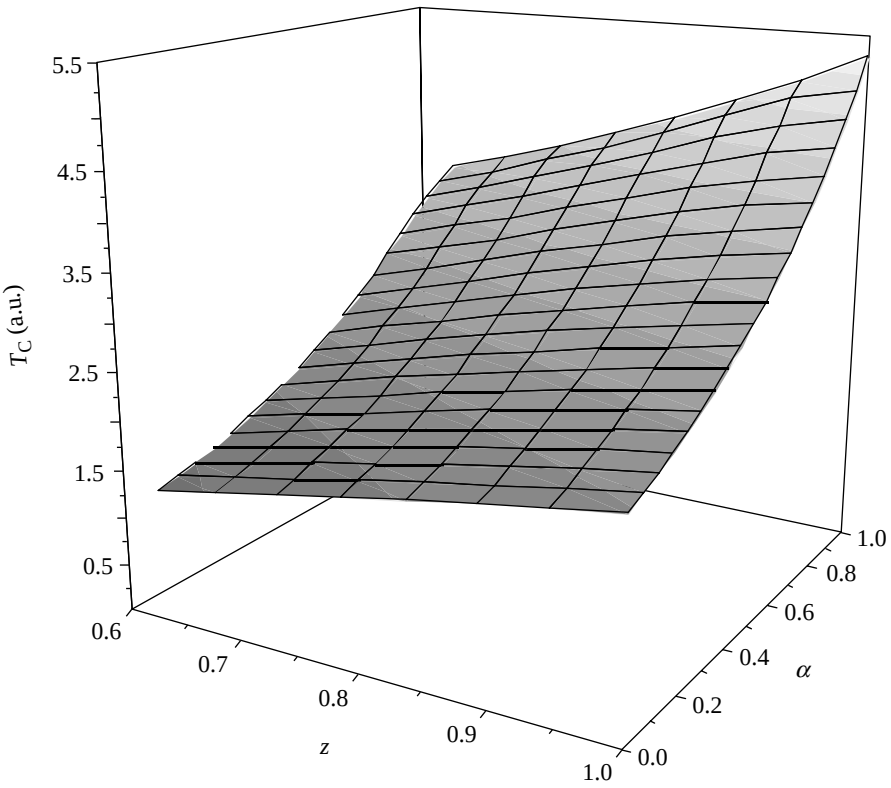

Figure 9. Computed values of T_C (in arbitrary units) when varying the stoichiometry z and the fraction α of vanadium (II) in the VCr system.

T_C varying between 295 and 376 K (above 100 °C) and various magnetizations at saturation (Hashimoto *et al.*, personal communication).

We report here some of our endeavours in dealing with: (i) the influence of (an)aerobic conditions; (ii) the stoichiometry, controlled by the addition of countercations; (iii) the nature of the counteranion; and (iv) the nature of the solvent (see Dujardin *et al.* 1998) using the above theoretical analysis.

(i) Prepared in aerobic conditions, the [VCr] system gives a crystalline dark green product $(V^{IV}O)_3[Cr^{III}(CN)_6]_2$ with a much lower T_C (110 K) (see Ferlay *et al.* 1999). The use of anaerobic conditions appears a necessary condition to avoid the oxidation of V^{II}, even if sol–gel procedures seem to limit it (see Holmes & Girolami 1999).

(ii) Concerning stoichiometry and countercations, there is a warning: the compound with the highest computed T_C, V/Cr = 1, corresponds to an antiferromagnet. Indeed, the antiparallel alignment of the neighbouring spins in the magnetically ordered phase leads to a resulting total magnetization M_T which is the difference between the magnetization arising from the subset of chromium ions M_{Cr} and the magnetization from the subset of vanadium ions, M_V:

$$M_T = |M_{Cr} - M_V|. \tag{3.1}$$

It is then necessary to explore the role of the stoichiometry, tuned by countercations such as Cs^+, and to compute systematically the magnetization to be sure not to have

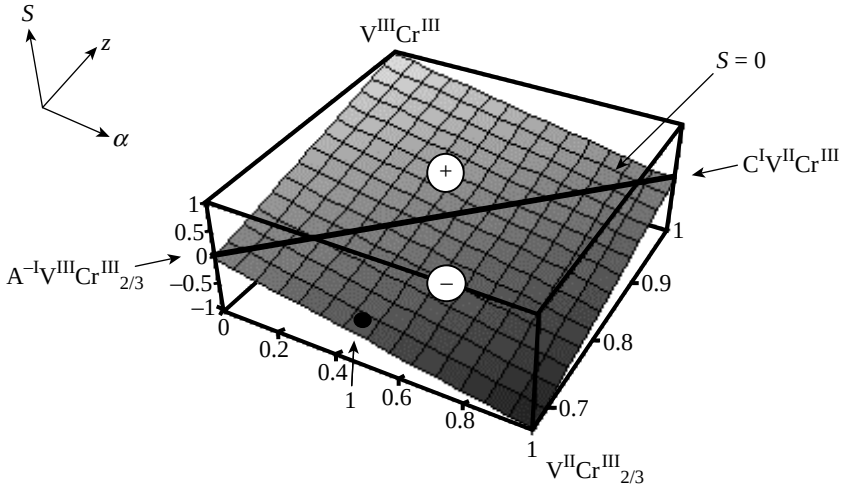

Figure 10. Variation of the spin values S versus z and α in mixed valency compounds, $C_y^{\mathrm{I}}\mathrm{V}_{\alpha}^{\mathrm{II}}\mathrm{V}_{1-\alpha}^{\mathrm{III}}[\mathrm{Cr}^{\mathrm{III}}(\mathrm{CN})_6]_z$, $n\mathrm{H_2O}$.

a true antiferromagnet by exact cancellation of the spins ($M_{\mathrm{Cr}} = M_{\mathrm{V}}$). In the case of the $C_1^{\mathrm{I}}\mathrm{V}_{\alpha}^{\mathrm{II}}\mathrm{V}_{(1-\alpha)}^{\mathrm{III}}[\mathrm{Cr}^{\mathrm{III}}(\mathrm{CN})_6]_z \cdot n\mathrm{H_2O}$ system,

$$M_{\mathrm{T}} = -(3z - \alpha - 2). \tag{3.2}$$

The corresponding plane is shown in figure 10, where α varies between 0 and 1 and z varies between $\frac{2}{3}$ and 1.

When $M_{\mathrm{Cr}} > M_{\mathrm{V}}$, the magnetic moments of the chromium ions are aligned parallel to an external applied field; when $M_{\mathrm{V}} > M_{\mathrm{Cr}}$, the magnetic moments of the vanadium ions now lie parallel to the field. We can verify that the first room-temperature magnet, with $M_{\mathrm{S}} = 0.15\mu_{\mathrm{B}}$, was close to the line $M_{\mathrm{T}} = 0$, shown in bold in figure 10! We can also use this new predicting tool to prepare new compounds with enhanced magnetization. The two compounds formulated,

$$\mathbf{A}: \quad \mathrm{V}_{0.45}^{\mathrm{II}}\mathrm{V}_{0.53}^{\mathrm{III}}(\mathrm{V}^{\mathrm{IV}}\mathrm{O})_{0.02}[\mathrm{Cr}(\mathrm{CN})_6]_{0.69}(\mathrm{SO}_4^{2-})_{0.23}(\mathrm{K_2SO_4})_{0.02} \cdot 3\mathrm{H_2O},$$

$$\mathbf{B}: \quad \mathrm{Cs}_{0.82}\mathrm{V}_{0.66}^{\mathrm{II}}(\mathrm{V}^{\mathrm{IV}}\mathrm{O})_{0.34}[\mathrm{Cr}(\mathrm{CN})_6]_{0.92}(\mathrm{SO}_4^{2-})_{0.20} \cdot 3 \cdot 6\mathrm{H_2O},$$

present similar T_{C} but a larger magnetization than in the first reported [VCr] ($0.36N_{\mathrm{A}}\beta$ for **A** and $0.42N_{\mathrm{A}}\beta$ for **B**) (see Dujardin *et al.* 1998). The calculated M_{T} value is positive for **A** ($M_{\mathrm{T}} = +0.36N_{\mathrm{A}}\beta$) and negative for **B** ($M_{\mathrm{T}} = -0.42N_{\mathrm{A}}\beta$). The absolute values are in good agreement with the experimental values but the sign of the two M_{T} values is opposite. This intriguing situation can be revealed amazingly by X-ray magnetic circular dichroism (XMCD), a new X-ray spectroscopy developed with synchrotron radiation, which is an element and orbital selective magnetic local probe, able to give direct information about the local magnetic properties of the photon absorber (direction and magnitude of the local magnetic moment) whatever the state of the sample (crystals, powders, etc.). Besides the usefulness of XMCD to

determine locally the spin orientation on each metal ion, the measurements explicitly showed

(1) the antiferromagnetic coupling between vanadium and chromium ions; and

(2) the change of the majority spin location caused by the modification of the chemical composition from vanadium in **A** to chromium in **B**.

The influence of the stoichiometry on the T_C has recently been beautifully shown (see Holmes & Girolami 1999), enabling T_C to reach 376 K in a compound formulated as $K^{I}V^{II}[Cr^{III}(CN)_6]$, displaying a weak magnetization, as expected.

(iii) and (iv) When looking at the structure (figure 2*c*), one realizes that vacancies and channels in Prussian blues can accommodate guest molecules: cations, as seen before, but also anions and solvent, which can either improve or compromise the short- and long-range structural organization of the material. We therefore varied the nature of the anions (I^-, SO_4^{2-}, Cl^-) and of the solvents (water, methanol, THF, etc.) under anaerobic conditions, according to the equation

$$3[V(H_2O)_6]A_2 + 2B_3[Cr(CN)_6] \xrightarrow{\text{solvent}} V_3[Cr(CN)_6]_2 \cdot xH_2O, \tag{3.3}$$

where A (anions) = I^- (weak Lewis base), SO_4^{2-} (weak Lewis base), Cl^- (stronger Lewis base), etc.; B = K^+, NH_4^+, NBu_4^+, etc.; and solvent = H_2O, MeOH, THF, DMSO, etc.

We obtained:

1 $V[Cr(CN)_6]_{0.73}(NBu_4^+)_{0.19}(I^-)_{0.03} \cdot 4H_2O$ (solvent, H_2O; starting materials, $(NBu_4)_3[Cr(CN)_3]$ and $[V(MeOH)_6]I_2$; $T_C = 326$ K);

2 $V[Cr(CN)_6]_{0.64}(NBu_4^+)_{0.04}(SO_4^{2-})_{0.15} \cdot 4 \cdot 4H_2O$ (solvent, H_2O; starting materials, $(NBu_4)_3[Cr(CN)_3]$ and $(NH_4)_2V(SO_4)_2 \cdot 6H_2O$; $T_C = 320$ K);

3 $V[Cr(CN)_6]_{0.69}(NBu_4^+)_{0.1}(Cl^-)_{0.14} \cdot 4H_2O$ (solvent, H_2O; starting materials: $(NBu_4)_3[Cr(CN)_3]$ and $VCl_2 \cdot 4H_2O$; $T_C = 308$ K).

We detected the Curie temperatures with a new device, which allowed the measurement of the permeability of the magnetic materials in their storage vessels. The T_C values obtained are indicated in figure 11. They are the same as those measured by SQUID.

In the IR spectra, we observe in the 2300–2000 cm^{-1} region two bands with different intensities for all compounds. The stronger band is centred around 2112 cm^{-1} and the weaker band is centred around 2162 cm^{-1}. We observe that the stronger band shifts to lower energy and the weaker band shifts to higher energy (ΔE is higher) when the compound has a smaller amount of V^{III} and its T_C is higher. Moreover, we observe that the weaker band not only shifts to higher energy (*ca.* 2170 cm^{-1}) but also its intensity increases when the compound is in a more oxidized state. We did not observe the band at 981 cm^{-1} corresponding to the $\nu_{as}V^{IV}{=}O$ stretching which confirms that there is no $V^{IV}{=}O$ in the compounds.

Counterions have large effects on T_C. Disorder in the Prussian blues' structures can be revealed at two levels: local order (coordination of anions which decreases the number of magnetic neighbours; distortion of the Cr—CN—V sequence, which decreases $|J|$); and long-range order (quality of the crystallization and size of the

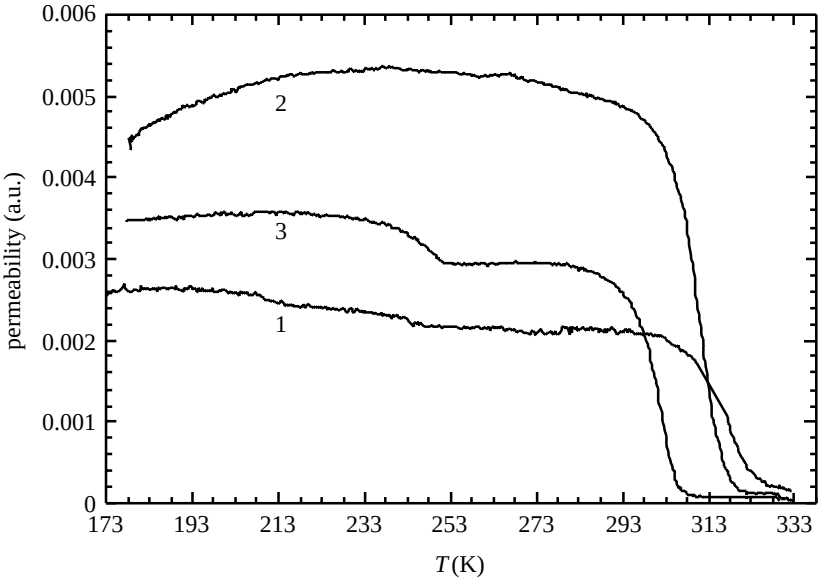

Figure 11. Permeability versus temperature measured for compounds **1**, **2** and **3**.

magnetic particles). The ions that do not distort the structures lead to better crystalline compounds with improved magnetic properties. The large size (NBu_4^+) and weakly coordinating ions, like I^-, induce less disorder and favour higher T_C.

We also carried out the reaction in organic solvents to avoid the oxidation of V^{II} by water and to study the influence of the solvent on the magnetic properties. In the same general conditions as for **1**, we got compounds **4** and **5** from reaction in methanol and THF, respectively:

4 $V[Cr(CN)_6]_{0.69}(I^-)_{0.03} \cdot 1.5MeOH$ (solvent, methanol; starting materials, $(NBu_4)_3[Cr(CN)_3]$ and $[V(MeOH)_6]I_2$; $T_C = 200$ K);

5 $V[Cr(CN)_6]_{0.68}(NBu_4^+)_{0.27}(I^-)_{0.33} \cdot 1.9H_2O$ (solvent, THF; starting materials, $(NBu_4)_3[Cr(CN)_3]$ and $[V(MeOH)_6]I_2$; $T_C = 290$ K).

Compounds **4** and **5** display the same IR bands as above. Figure 12 indicates the T_C of **1**, **4** and **5**.

We propose that the changes in the magnetic properties are mainly due to the changes in the structure induced by the kinetics of solvent exchange in $[V(solvent)_6]^{2+}$ (see Lincoln & Merbach 1995): when the exchange is fast, in water, the substitution of the solvent molecules by CN^- around V^{II} is more effective, the number of magnetic neighbours increases and so does T_C. In methanol, the kinetics of exchange is slow, hence the poor quality of the magnetism. In THF, with faster kinetics, the T_C of the bright blue compound reaches room temperature (17 °C).

4. Prospects

We give here three directions that we are exploring, among others: magnetic devices; magneto-optical properties; and conditions to get single-molecule magnets at room temperature.

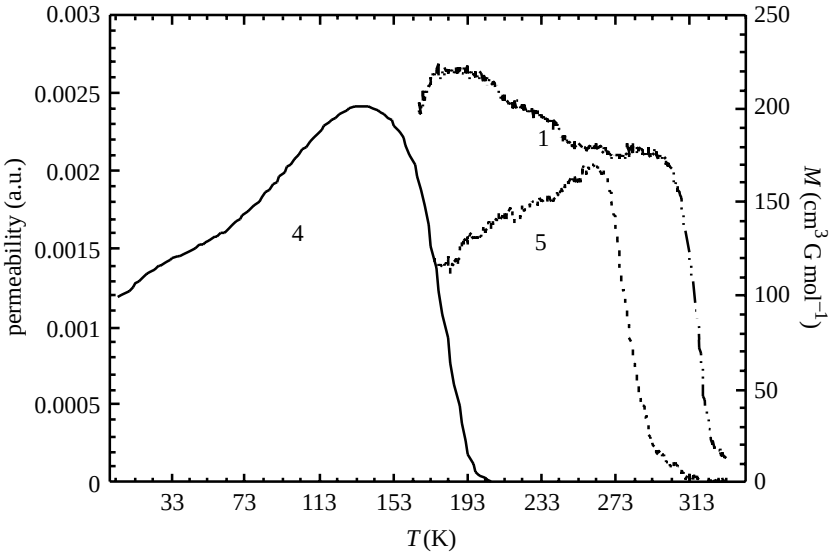

Figure 12. Permeability (compounds **1** and **5**) and magnetization (compound **4**) versus temperature.

(*a*) *Devices from room-temperature magnets*

A molecule-based magnet, such as our [VCr] system, is a useful tool to illustrate easily, near room temperature, what a Curie temperature is. Figure 13 displays a demonstrator designed for this purpose.

[VCr] is sealed in a glass vessel under argon and suspended at the bottom of a pendulum (equilibrium, position (2) in absence of permanent magnet). It is then cycled between its two magnetic states: the three-dimensional ordered ferrimagnetic state, when $T < T_C$; and the paramagnetic state, when $T > T_C$. The three steps are as follows.

(i) The 'room-temperature magnet' is cold ($T < T_C$, ferrimagnetic state). It is attracted ($\rightarrow$) by the permanent magnet and deviates from the vertical direction towards position (1). The light beam is focused at position (1) above the permanent magnet. The light heats the sample.

(ii) When $T > T_C$, the hot 'room-temperature magnet' is in the paramagnetic state. It is no longer attracted and moves away from the magnet ($\leftarrow$) under the influence of its own weight. It is then air cooled and its temperature decreases.

(iii) When $T < T_C$, the cold 'room-temperature magnet' is attracted again by the permanent magnet ($\rightarrow$) and comes back to position (1). The system is ready for a new oscillation.

The demonstrator works well in our laboratory: millions of cycles have been accomplished without any fatigue. The demonstrator is an example of a thermodynamical machine working between two energy reservoirs with close temperatures (sun and shadow) allowing the conversion of light into mechanical energy. We are exploring other practical applications: thermal probes, magnetic switches, etc.

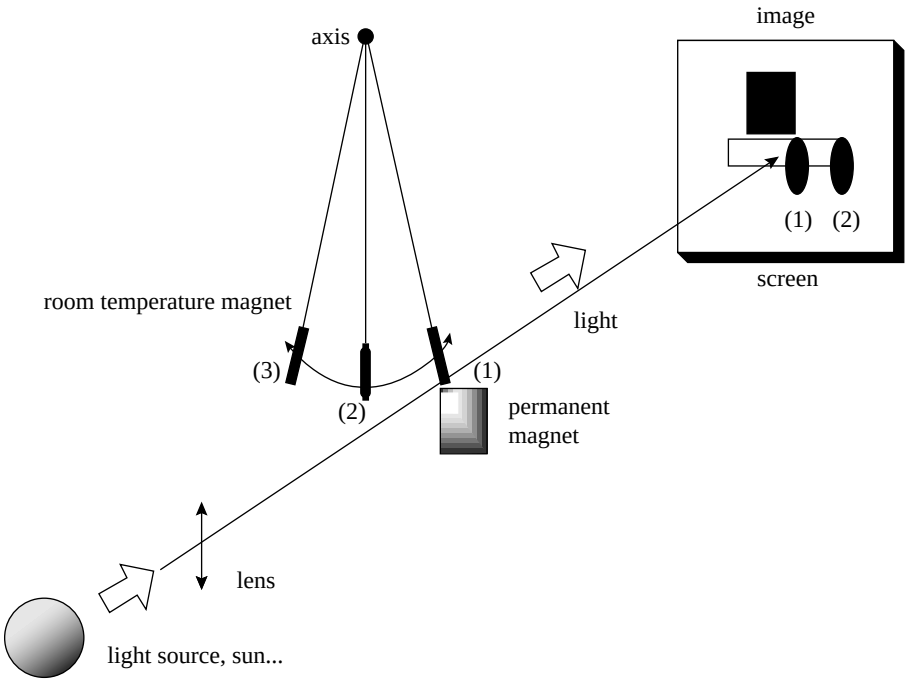

Figure 13. Demonstrator using the properties of a room-temperature magnet to transform light into mechanical energy.

(*b*) *Thin layers*

Magnetic Prussian blue analogues display bright colours and transparency, among other interesting properties. To exploit these optical properties it is useful to prepare thin films, and a 1 μm thick film of vanadium–chromium magnet is indeed quite transparent. The best way to prepare thin films of these materials is electrochemical synthesis and various films have been prepared from hexacyanoferrates in recent years. To obtain [VCr] thin films, experimental conditions are extensively modified. One actually wants to produce and to stabilize the highly oxidizable ions. Thus, strongly negative potentials are applied at the working transparent semiconducting electrode. The deposition of the [VCr] film is obtained from aqueous solutions of $[Cr^{III}(CN)_6]^{3-}$ and V^{III} at fixed potential or by cycling the potential.

In passing, we point to a further interesting property of [VCr] thin films, in that they also exhibit electrochromism. The way is open for the preparation of electrochromic room-temperature magnets.

The magnetization of a transparent magnetic film, protected by a transparent glass cover, can then be probed by measuring the Faraday effect, corresponding to spin-dependent modifications of the polarization of the transmitted light. Spectroscopic measurements in the UV–vis range reveal information about the magnetization of the sample and, moreover, about its electronic structure. Moreover, observing the Faraday effect at room temperature in these compounds is the first step in demonstrating that these materials can be used in magneto-optical information storage. We succeeded in obtaining for the first time on a [VCr] room-temperature magnet a magneto-optical signal at room temperature through a transparent semiconducting

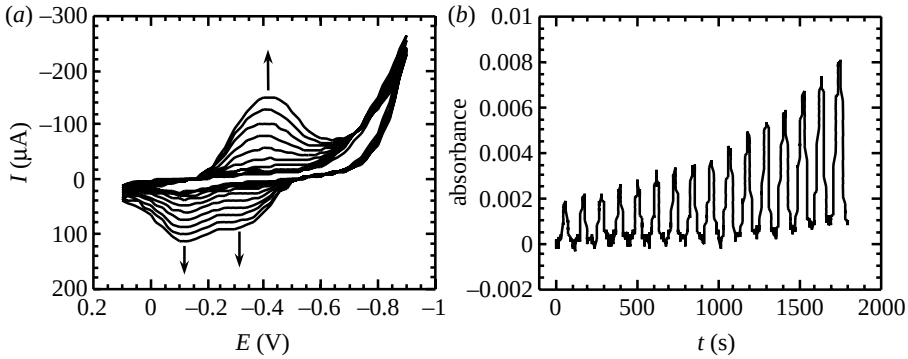

Figure 14. Cyclovoltammograms and electrochromism during the deposition of thin layer [VCr] by cycling the applied potential.

electrode. Further studies are needed to control the purity and the homogeneity of the layers, and to correlate the magneto-optical effects to the local magnetization of vanadium and chromium. They are underway, in a very promising area.

(*c*) *Towards room-temperature single-molecule magnets?*

The enhancement of the T_C values in Prussian blue magnets relies on the control of the interaction between the spin carriers. A brand new direction appeared some years ago when Sessoli *et al*. (1993) characterized the behaviour of a single-molecule magnet: a uniaxial anisotropic molecule presenting a ground state with a spin S and a zero-field splitting D displays an anisotropy barrier $E_a = DS_z^2$ and behaves as a magnet when $kT \ll E_a$. If the challenge in this field is the synthesis of a single-molecule magnet at room temperature, two conditions must be fulfilled: (i) the population of the high spin ground state at room temperature (and an interaction constant between the paramagnetic centres at *ca*. 400 K); and (ii) a uniaxial anisotropic barrier $E_a = DS_z^2$ larger than the thermal quantum at room temperature, i.e. *ca*. 400 K. The later condition can be reached, for example, with a total spin $S = 20$ and an anisotropy of the ground state $D = 1$ K. The challenge is difficult but not completely impossible to overcome. We are working in two directions: (i) the enhancement of the molecular spin, and we arrive at $S = \frac{27}{2}$ (see Mallah *et al*. 1995; Scuiller *et al*. 1996); and (ii) the improvement of the anisotropy of the system (see Scuiller 1999).

5. Conclusion

We have tried to show, through different examples essentially chosen from our own chemistry, that looking at old systems with new concepts can give rise to new systems, new properties and new applications. It is impossible to quote in a short text devoted to room-temperature magnets all the recent endeavours using cyanometallate precursors to build magnetic systems from zero to three dimensions. Bimetallic cyanide boxes and superboxes, complex frameworks using less symmetrical precursors than the hexacyano anions, thin layers, photomagnetic and multifunctional systems are appearing or near completion. We can expect in the near future important achieve-

ments in this field, where the flexibility of molecular precursors combines with the versatility of solid-state chemistry to build the new solid.

We thank the European Community (grants ERBCHRXCT92080, ERBFMBICT 972644 and ERBFMRXCT980181) and the European Science Foundation for financial support ('Molecular Magnets' Programme).

References

Babel, D. 1986 *Comments. Inorg. Chem.* **5**, 285.

Charlot, M. F. & Kahn, O. 1980 *Nouv. J. Chim.* **4**, 567.

Dujardin, E., Ferlay, S., Phan, X., Cartier dit Moulin, C., Sainctavit, P., Baudelet, F., Dartyge, E., Veillet, P. & Verdaguer, M. 1998 *J. Am. Chem. Soc.* **120**, 11 347.

Dunbar, K. R. & Heintz, R. A. 1997 In *Progress in inorganic chemistry* (ed. D. K. Kenneth), vol. 45, p. 282. Wiley.

Ferlay, S., Mallah, T., Ouahès, R., Veillet, P. & Verdaguer, M. 1995 *Nature* **378**, 701.

Ferlay, S., Mallah, T., Ouahès, R., Veillet, P. & Verdaguer, M. 1999 *Inorg. Chem.* **38**, 229.

Gadet, V., Mallah, T., Castro, I., Veillet, P. & Verdaguer, M. 1992 *J. Am. Chem. Soc.* **114**, 9213.

Gatteschi, D., Kahn, O., Miller, J. S. & Palacio, F. (eds) 1991 *Molecular magnetic materials.* NATO ASI Series E, vol. 198. Dordrecht: Kluwer.

Girerd, J. J., Journeaux, Y. & Kahn, O. 1981 *Chem. Phys. Lett.* **82**, 534.

Goodenough, J. B. 1963 *Magnetism and the chemical bond.* New York: Interscience.

Güdel, H. U. 1985 In *Magneto-structural correlation in exchange coupled systems* (ed. R. D. Willett, D. Gatteschi & O. Kahn). NATO ASI Series, p. 329. Dordrecht: Reidel.

Hay, P. J., Thibeault, J. C. & Hoffmann, R. 1975 *J. Am. Chem. Soc.* **97**, 4884.

Herpin, A. 1968 *Théorie du magnétisme.* Saclay: INSTN-PUF.

Holmes, S. M. & Girolami, S. G. 1999 *J. Am. Chem. Soc.* **121**, 5593.

Ito, A., Suenaga, M. & Ono, K. 1968 *J. Chem. Phys.* **48**, 3597.

Kahn, O. 1993 *Molecular magnetism.* New York: VCH.

Landrum, G. A. 1992 YAeHMOP: yet another extended Hückel molecular package. URL: http://overlap.chem.cornell.edu:8080/yaehmop.html.

Larionova, J., Sanchiz, J., Gohlen, S., Ouahab, L. & Kahn, O. 1998 *Chem. Commun.*, p. 953.

Lincoln, S. F. & Merbach, A. E. 1995 *Adv. Inorg. Chem.* **42**, 1.

Ludi, A. & Güdel, H. U. 1973 *Struct. Bonding* **14**, 1.

Mallah, T., Thiébaut, S., Verdaguer, M. & Veillet, P. 1993 *Science* **262**, 1554.

Mallah, T., Auberger, C., Verdaguer, M. & Veillet, P. 1995 *J. Chem. Soc. Chem. Commun.*, p. 61.

Manriquez, J. M., Yee, G. T., McLean, R. S., Epstein, A. J. & Miller, J. S. 1991 *Science* **252**, 1415.

Miller, J. S. & Dougherty, D. A. (eds) 1989 *Proc. Conf. on Ferromagnetic and High Spin Molecular Based Materials. Mol Cryst. Liq. Cryst.* **176**.

Néel, L. 1948 *Ann. Phys. Paris* **3**, 137.

Scuiller, A. 1999 PhD thesis, Université Pierre et Marie Curie, Paris.

Scuiller, A, Mallah, T., Nivorozkhin, A., Verdaguer, M. & Veillet, P. 1996 *New J. Chem.* **20**, 1.

Sessoli, R., Tsai, H.-L., Schake, A. R., Wang, S., Vincent, J. B., Folting, K., Gatteschi, D., Christou, G. & Hendrickson, D. N. 1993 *J. Am. Chem. Soc.* **115**, 1804.